non-metal was indicated by an increase or decrease in E_F on their formation.

Acknowledgment. The authors are indebted to J. W. Anderegg for the high-quality photoelectron spectra and to H. F. Franzen and B. N. Harmon for helpful and informative discussions.

Registry No. ZrCl, 14989-34-5; $ZrClD_{0.5}$, 87206-68-6; ZrClH, 60921-39-3; ZrBr, 31483-18-8; $ZrBrH_{0.5}$, 60967-29-5; ZrBrH, 60921-40-6.

Contribution from Ames Laboratory—DOE[1] and the Department of Chemistry, Iowa State University, Ames, Iowa 50011

Synthesis and Characterization of Oxide Interstitial Derivatives of Zirconium Monochloride and Monobromide

LINDA M. SEAVERSON and JOHN D. CORBETT*

Received February 14, 1983

The reactions of ZrO_2 with double-metal-layered ZrCl and ZrBr at ~980 °C and with Zr metal at 930 °C have been studied with the aid of high-resolution (Guinier) powder pattern data. The products of the first reaction are $ZrX(O_y)$, an expanded ZrX structure, and $Zr(O_x)$ from solution of ZrO_2 in the metal, viz., $ZrX + nZrO_2 = ZrX(O_y) + nZr(O_x)$. The oxygen composition of both products (y, x) varies continuously up to the point of ZrO_2 saturation where n, y, and x are respectively 0.27 (1), 0.43 (2), and 0.42 for chloride and 0.22 (2), ~0.35, and ~0.42 for bromide. Single-crystal X-ray results for $ZrBrO_{\sim 0.23}$, $ZrClO_{0.29}$, and $ZrClO_{0.43}$ establish the retention of the basic ZrX structure ($R\bar{3}m$) and the concentration of oxygen, which is distributed randomly in the distorted tetrahedral interstices between the zirconium layers. The last named composition (a = 3.4984 (2) Å, c = 27.065 (4) Å) is in equilibrium with ZrO_2 and gave a refined structure with R = 0.046 and R_w = 0.056 for 141 independent reflections with $2\theta \leq 59.9°$. UPS measurements show that the chloride oxide is still metallic. Attempts to achieve analogous products from reactions between ZrCl and ZrC, ZrN, ZrF_4, or $Zr_{1+x}S$ and diverse attempts to intercalate ZrCl were unsuccessful. The mean Zr–O distance in $ZrClO_{0.43}$, 2.07 Å, is close to that found in tetragonal and monoclinic ZrO_2 and to the sum of conventional crystal radii, in agreement with the general observation that significant screening is not provided by the delocalized electrons. The size of the available interstices in ZrX and the metal appear to be important factors in oxide substitution in the T_d and O_h sites, respectively, and in the course of the other ZrX reactions studied. Fluoride substitution evidently fails because of the absence of an analogous $Zr(F_x)$ metal product.

Introduction

The novel structures of the zirconium monohalides ZrCl and ZrBr provide a basically two-dimensional metal-like substrate for study. These phases consist of cubic-close-packed layers of zirconium and halide atoms stacked in pairs to yield the sequence X–Zr–Zr–X[2-4] with relative orientations AbcA. These tightly bound four-layer slabs are in turn weakly bound in the order ABCA (designating outer halogen layers only) in ZrCl or ACBA in ZrBr. The strength of the metal–metal interactions are revealed by the short metal–metal distances, for example, three at 3.09 Å in the other layer and six at 3.43 Å in the same layer in ZrCl vs. comparable distances of 3.18 Å and 3.23 Å in the hcp metal. The d orbitals are strongly split by these interactions, but the materials are still metallic[4-7] and graphite-like[8] and are therefore candidates for interesting reactions and products. Thus, both substrates take up hydrogen with small changes in layering to form $ZrXH_{0.5}$ and ZrXH in which hydrogen is in tetrahedral interstices as it is in ZrH_{2-x} (defect fluorite structure).[9-11] Other studies of the monohalides include their use as synthetic intermediates[12,13] and unsuccessful attempts at intercalation with metal ions.[4] One particularly interesting observation by Daake[14] was that the lattice constants of ZrCl and ZrBr increase 1–2% on reaction with ZrO_2 at 850 °C. The change was suggested to arise from loss of electron density between the zirconium layers accompanying the substitution of oxide in the halide layers, viz., $ZrX_{1-n}O_n$.

The present article reports an investigation of these ZrX–ZrO_2 reactions and products, especially the identification of the reaction stoichiometry and the structure and photoelectron spectra of the oxidized ZrX phase. Analogous reactions of other non-metals with ZrX and further attempts to intercalate ZrCl are also described.

Experimental Section

Syntheses. The moderate air and moisture sensitivity of the reactants and products even at room temperature dictates the use of typical drybox and vacuum techniques. The dryboxes were constantly purged with dry N_2 that recirculated through a column of molecular

(1) Operated for the U.S. Department of Energy by Iowa State University under Contract No. W-7405-Eng-82. This research was supported by the Office of Basic Energy Sciences, Materials Sciences Division.
(2) Troyanov, S. I. *Moscow Univ. Chem. Bull. (Engl. Transl.)* **1973**, *28*, 89.
(3) Adolphson, D. G.; Corbett, J. D. *Inorg. Chem.* **1976**, *15*, 1820.
(4) Daake, R. L.; Corbett, J. D. *Inorg. Chem.* **1977**, *16*, 2029.
(5) Troyanov, S. I.; Tsirel'nikov, V. I. *Russ. J. Inorg. Chem. (Engl. Transl.)* **1970**, *15*, 1762.
(6) Marchiando, J. F.; Harmon, B. N.; Liu, S. H. *Physica B+C (Amsterdam)* **1980**, *99B+C*, 259.
(7) Corbett, J. D.; Anderegg, J. W. *Inorg. Chem.* **1980**, *19*, 3822.
(8) Dean, R. S. *Ind. Lab.* **1959**, *10*, 45.
(9) Struss, A. W.; Corbett, J. D. *Inorg. Chem.* **1977**, *16*, 360.
(10) Marek, H. S.; Corbett, J. D.; Daake, R. L. *J. Less-Common Met.* **1983**, *89*, 243.
(11) Corbett, J. D.; Marek, H. S. *Inorg. Chem.*, preceding paper in this issue.
(12) Daake, R. L.; Corbett, J. D. *Inorg. Chem.* **1978**, *17*, 1192.
(13) Cisar, A. J.; Corbett, J. D.; Daake, R. L. *Inorg. Chem.* **1979**, *18*, 836.
(14) Daake, R. L. Ph.D. Dissertation, Iowa State University, 1976.

0020-1669/83/1322-3202$01.50/0

sieves. This and a tray of P_2O_5 typically reduced the H_2O content to 1–4 ppm. Because the materials are very reactive with air, moisture, and many conventional containers at elevated temperatures, the customary[3,4,14] welded tantalum containers (0.95-cm o.d. × ~3.5 cm) in fused-silica jackets were employed. The absence of reaction between Ta and ZrO_2 was indicated by $\Delta G°_{298}$ = 332 kcal for $4Ta + 5ZrO_2 \rightarrow 5Zr + 2Ta_2O_5$,[15] and no evidence of any interaction was observed. Chromel–alumel thermocouples attached on the outside of the jacket at the extremes of the Ta tubes monitored the temperature and any gradients.

The zirconium monohalides (<500 ppm of Hf) used were prepared by the method developed by Daake.[4] ZrO_2 (<200 ppm of Hf) was prepared by passing an air stream over $ZrOCl_2 \cdot 8H_2O$ at either 600 °C for 1 h or 300–350 °C for 4–6 h. X-ray fluorescence found 1.9 ± 0.4 wt % Cl (Cl:Zr = 0.07) in this ZrO_2 after calibration with standards while spectrophotometric analysis after heating with concentrated NaOH at 80 °C for 4 h gave 0.37 ± 0.1 wt % Cl (Cl/Zr = 0.016). Samples of powdered Zr were obtained by decomposition of ZrH_{2-x} under high vacuum at 575 °C. Standard samples of $Zr(O_x)$ were prepared by equilibration in Ta of weighted amounts of ZrO_2 and powdered Zr at 930 °C for 14 days.

ZrN and ZrC (Cerac, Inc.) each containing <200 ppm of Hf were degassed at 250 °C under dynamic vacuum in an open Ta tube for 24 h. The ZrF_4[16] was purified by vacuum sublimation in tantalum at 600 °C. Emission spectroscopy found no impurities other than a trace of iron and titanium. $ZrS_{0.867}$ (WC type), $ZrS_{1.29}$ (NaCl type), and ZrS_2 obtained from Franzen and co-workers had been prepared as described.[17,18]

Desired masses of ZrX and ZrO_2 (or ZrN, ZrS_y, ZrF_4, or ZrC) and sometimes Zr powder, generally totalling less than 300 mg, were weighed in separate glass vials, ground together, and enclosed in a Ta tube in the drybox, after which the crimped end of the container was heliarc welded. The majority of the halide reactions were heated at 890–1025 °C for 2 weeks with little temperature gradient along the tube. The minimum times necessary for complete $ZrX–ZrO_2$ reaction were generally between 10 days at 1025 °C and 14 days at 890 °C (for $ZrX + 0.11ZrO_2$). Incomplete reaction of $ZrCl + 0.23ZrO_2$ was observed in 6 days at 1016 °C. Reactions were normally cooled within the furnace by shutting off the power, although in a few cases a motorized potentiometer was attached to the controller's thermocouple to obtain cooling at 1–4 °C h^{-1}. The lattice dimensions of the products showed no dependence on equilibration temperature within the stated range, although these were slightly ($<3\sigma$) higher when the reaction products had been cooled slowly. The tantalum containers were bulged after the reactions, the typical crimped and welded end being expanded nearly back to the original diameter. Study of the reactions of ZrS_2, even in the presence of excess metal, was limited to temperatures no higher than 850 °C by severe attack of the Ta container. Compositions near ZrS were reacted with ZrCl either for 14 days at 600 °C after prior pressing of the reactants to 8000 psi within the sealed container or for 14 days at 970 °C. ZrN, ZrC, and ZrF_4 were each reacted with ZrCl for 2–3 weeks at 910–1000 °C.

Characterization. The Guinier powder pattern technique[19] was extensively used for phase identification and lattice constant determination. The sample mounting and data treatment methods have been described before.[4,13] For calibration, a quadratic function in film position was fit to the 2θ values of an internal Si standard. Standard least-squares methods were used to obtain lattice constants from indexed patterns. The ZrCl structure type characteristically gives greater line broadening from grinding than does ZrBr unless subsequent annealing is included.[4] This persists to a reduced degree with the oxide derivatives and causes generally higher uncertainties in lattice dimensions, especially in *c*.

As a first check on a reaction, the Guinier powder pattern of the products was visually compared with a standard pattern for ZrX. If no noticeable shift in the reflection positions or intensities or addition of new reflections resulted, the extent of reaction was considered so minimal that it could be termed unsuccessful, and the lattice dimensions were not determined. The 110 and 113 reflections of ZrCl are particularly sensitive to changes in the lattice dimensions.

Table I. Intercalation Attempts with ZrCl

reactants	P, atm	T, °C	time, days	products[a]
NH_3(g)	10	20	3	nr
NH_3(g)	8–9	300	5	$ZrClH_{0.5}$, ZrClH, NH_4Cl
NH_3(g)	10	260	0.6	nr
NH_3(g)	10	388	0.6	NH_4Cl
pyridine		190	2	white, $ZrClH_{0.5}$
CO	68	170	0.5	nr
n-butyllithium		20	5	nr
n-butyllithium		60	5	white
Li/NH_3(l)		−33	0.4	nr
K/NH_3(l)		−33	0.4	nr
LiCl, $ZrCl_4$, Zr[b]		700/618	9	LiCl
LiCl, Zr		730	8	LiCl
CsCl, Zr		780/670	11	CsCl
NaCl, $ZrCl_4$, Zr (pwd)		400 → 930	11	NaCl
LiCl, Li		550	8	LiCl
Li		850	1	Zr + soft plates[b,c]

[a] In addition to ZrCl with unshifted pattern; nr = no reaction. [b] No ZrCl. [c] Four unidentified reflections.

Photoelectron spectra, both XPS (Al Kα, 1486.6 eV) and UPS (He I, 21.21 eV), were obtained on an AEI Model ES200B instrument coupled to a Nicolet 1180 microcomputer. Samples were pressed into In strips or onto adhesive tape in the attached drybox (H_2O and O_2 <1 ppm). Three to thirteen scans were collected per examination with 512 channels and with a monochromator in use for the XPS data collection. The C 1s level at 285.0 eV was used as reference. No charging was noted.

Suitable single crystals in the form of thin plates were mounted in 0.3-mm thin-walled capillaries in a drybox under 15-power magnification. Oscillation and zero- and first-level Weissenberg photographs were used to establish their singularity and diffracting ability and the absence of any intergrowth or superstructure.

Four single-crystal data sets were collected on $ZrX(O_y)$ products of $ZrX–ZrO_2$ reactions from crystals about 0.15 × 0.15 × 0.005 mm for the chlorides and about 20 times thicker for the bromide. The measurements utilized either a Datex or Ames Laboratory diffractometer interfaced to a PDP 15 computer and Mo Kα radiation (λ = 0.709 26 Å) monochromatized by a graphite single crystal. The intensities of three standard reflections were monitored every 75 reflections to check for instrument and crystal stability with no evidence of change. In each case four octants of data were collected with no restrictions. Final lattice dimensions were obtained by a least-squares fit of 13 or 14 reflections ($25° < 2\theta < 40°$), each of which was tuned on both Friedel-related peaks. Examination of the data sets revealed that the systematic extinction condition $-h + k + l = 3n$ always applied, and $R\bar{3}m$ (No. 166), the space group of ZrCl and ZrBr, was chosen. An empirical absorption correction was carried out on each by using diffractometer ϕ-scan data tuned on the peak every 10° and the program ABSN[20] (μ = 64.9 cm^{-1} for $ZrCl(O_y)$ and 251 cm^{-1} for $ZrBr(O_y)$[21]). Averaging the observed reflections yielded the independent data sets with no reflections eliminated by a cutoff of 6σ from the average. Structure factor calculations and full-matrix least-squares refinements were carried out with the program ALLS[22] while Fourier series calculations were done with FOUR.[23]

Intercalation Reactions. Although some attempts at intercalation have been reported before,[4] a more extensive survey was accomplished in the present work. The negative results are summarized in Table I. For NH_3(g) reactions a sample of ZrCl was placed in a fused silica pail that easily slipped into and out of a stainless-steel bomb. The detection of NH_4Cl suggests unidentified zirconium amide products

(15) "Selected Values of Chemical Thermodynamic Properties". *NBS Tech. Note (U.S.)* **1971**, No. 270-5.
(16) Fukutomi, M.; Corbett, J. D. *J. Less-Common Met.* **1977**, *55*, 125.
(17) Conrad, B. R.; Franzen, H. F. *High Temp. Sci.* **1970**, *3*, 49.
(18) Conrad, B. R.; Franzen, H. F. In "The Chemistry of Extended Defects in Non-Metallic Solids"; North-Holland Publishing Co.: Amsterdam, 1970; p 207.
(19) Westman, S.; Magneli, A. *Acta Chem. Scand.* **1957**, *11*, 1587.
(20) Karcher, B. Ph.D. Dissertation, Iowa State University, 1981.
(21) "International Tables for X-ray Crystallography", 2nd ed.; Kynoch Press: Birmingham, England, 1962; Vol. III, p 166.
(22) Lapp, R. L.; Jacobson, R. A. unpublished research, Iowa State University, 1979.
(23) Powell, D. R.; Jacobson, R. A., unpublished research, Iowa State University, 1979.

Table II. Lattice Constants (Å) for Products of $ZrX-nZrO_2$ Reactions[a]

	$ZrX(O_y)$ phase			$Zr(O_x)$ phase		
n	a	c	N^b	a	c	N^b
			ZrCl			
0[c]	3.4233 (5)	26.693 (3)	10	3.2323 (7)[d]	5.1477 (7)[d]	9
0	3.423 (5)	26.65 (7)	6	3.2340 (6)	5.1487 (13)	10
0.08	3.4542 (7)	26.797 (13)	9	3.2483 (5)	5.2074 (9)	13
0.11	3.4623 (8)	26.902 (11)	10	3.2481 (1)	5.2069 (2)	9
0.20	3.4829 (5)	26.992 (7)	14	3.2421 (4)	5.2069 (8)	11
0.22	3.4814 (5)	26.973 (9)	13	3.2422 (4)	5.2061 (7)	13
0.23	3.4807 (6)	26.981 (9)	13	3.2431 (2)	5.2073 (4)	13
0.25	3.4920 (5)	27.026 (8)	10	3.2398 (4)	5.2061 (8)	10
0.26	3.4940 (5)	27.060 (1)	16	3.2399 (3)	5.2064 (6)	13
0.33	3.4905 (5)	27.050 (9)	14	3.2390 (1)	5.2070 (3)	8
0.43	3.4955 (4)	27.032 (11)	9	3.2406 (4)	5.2096 (7)	5
0.67	3.4960 (6)	27.049 (9)	11			
0.67[e]	3.4984 (2)	27.065 (4)	9[f]			
	3.4993 (5)	27.079 (10)	10			
			ZrBr			
0	3.5031 (3)	28.071 (3)	23			
0	3.5064 (2)	28.068 (2)	29	3.2340 (6)	5.1487 (13)	10
0.11	3.5402 (2)	28.313 (3)	28	3.2475 (2)	5.2076 (4)	9
0.13	3.5517 (2)	28.384 (5)	21	3.2463 (3)	5.2180 (6)	7
0.15[e]	3.5594 (4)	28.418 (5)	13[f]	3.2466 (3)	5.2174 (7)	11
	3.5541 (3)	28.412 (4)	28			
0.18	3.5561 (2)	28.419 (4)	22	3.2455 (2)	5.2225 (9)	7
0.23	3.5581 (3)	28.434 (4)	25	3.2441 (3)	5.2176 (8)	7
0.67[e]	3.5587 (3)	28.425 (6)	22	3.239 (2)	5.216 (8)	8

[a] From Guinier powder data of unannealed product unless otherwise noted. [b] Number of reflections used in refinement. [c] ZrCl annealed after grinding; from ref 4. [d] Pure metal; ref 25. [e] Reaction cooled slowly. [f] Reflections from single crystal tuned on diffractometer.

were also formed. The pyridine attempts involved sealing ZrCl plus dry pyridine in a Pyrex tube. The first *n*-butyllithium reaction was carried out as described by Dines[24] utilizing the 0.26 M reagent in hexane. The second used 1.6 M *n*-butyllithium in an evacuated and sealed Pyrex tube.

Results

$ZrX-ZrO_2$ Reactions. The products of these reactions are microcrystalline powders or sintered clumps that are dark gray to very dark olive in color for the chloride and bronze for the bromide. Larger hexagonal plates were found as the amount of ZrO_2 approached a reaction limit, and these better approached singularity when the sample was cooled within a furnace of larger heat capacity (Lindberg) by turning the power off. Many single crystals were found when three reactions were terminated by cooling at 1–4 °C h^{-1}; more reasonable, intermediate cooling rates would probably also work.

Guinier powder patterns of the products of the reaction of ZrX with increasing amounts of ZrO_2 showed an expanded ZrX lattice ($ZrX(O_y)$) with negligible intensity changes and no new lines but with the typically broad lines sharpened (so lattice dimension accuracy improved). The powder data also exhibited an expanded pattern of the hcp metal caused by oxygen solution in zirconium metal ($Zr(O_x)$) and, beyond a stoichiometric limit, the monoclinic ZrO_2 pattern. Thus, the general reaction is evidently

$$ZrX + nZrO_2 = ZrX(O_y) + nZr(O_x) \qquad (1)$$

x and y being variable from zero to some limit, with provisional assumptions of the retention of the 1:1 stoichiometry for Zr:X in the layered product and the absence of a significant solution of X in the metallic $Zr(O_x)$. Of course there is also a conservation condition, $2n = y + nx$. The following investigations provide independent assessments of the values of n, y, and x in the chloride system and of n with the bromide.

Table II lists the lattice constants of the equilibrium trigonal (rhombohedral) $ZrX(O_y)$ and hexagonal $Zr(O_x)$ phases obtained from a series of reactions with various values of n, the initial molar ratio of ZrO_2 to ZrX. Figures 1 and 2 show the dependencies of the a and c dimensions on n for the $ZrCl(O_y)$

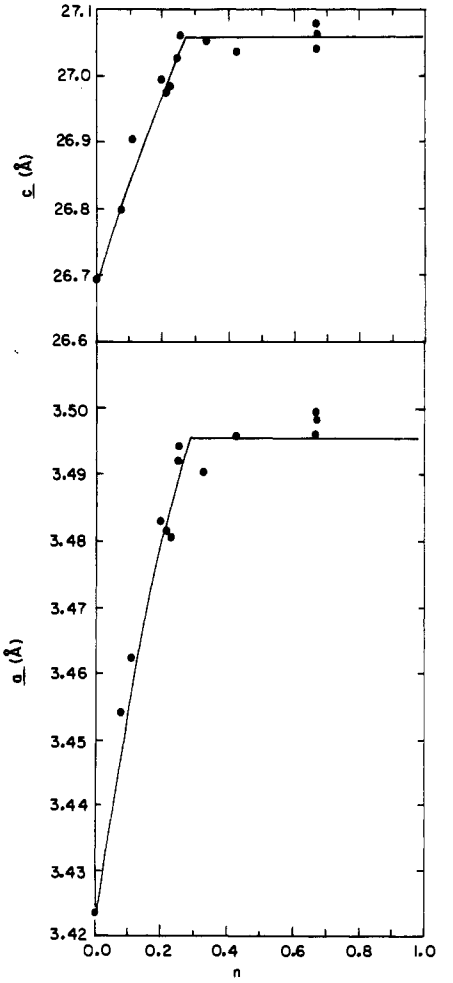

Figure 1. Lattice dimensions of the $ZrCl(O_y)$ product as a function of n for the reaction $ZrCl + nZrO_2 = ZrCl(O_y) + nZr(O_x)$.

(24) Dines, M. B. *Mater. Res. Bull.* **1975**, *10*, 287.

Table III. Average Lattice Parameters of ZrO_2-Saturated Phases (Å)

phase	n^a	a	c	$N(a), N(c)^b$	Δa,[c] %	Δc, %
$ZrCl(O_{satd})$	0.27 ± 0.01	3.4956 (5)	27.06 (1)	6, 6	2.11	1.4
$ZrBr(O_{satd})$	0.22 ± 0.02	3.5584 (4)	28.430 (7)	2, 2	1.53	1.26
$Zr(O_{satd})$						
930 °C[d]		3.2428 (4)	5.2010 (7)	3, 3		
800 °C[e]		3.2443	5.2030	4, 4	0.05	−0.04
$+ZrCl(O_{satd})$		3.2398 (4)	5.2077 (7)	3, 9	−0.09	0.13
$+ZrBr(O_{satd})$		3.239 (2)	5.2189 (9)	1, 4	−0.1	0.34

[a] Moles of ZrO_2/mol of ZrCl at saturation. [b] Number of values averaged; from Figures 1–4. [c] Relative to binary ZrX (ref 4) or ZrO_x (this work). [d] This work. [e] Reference 25.

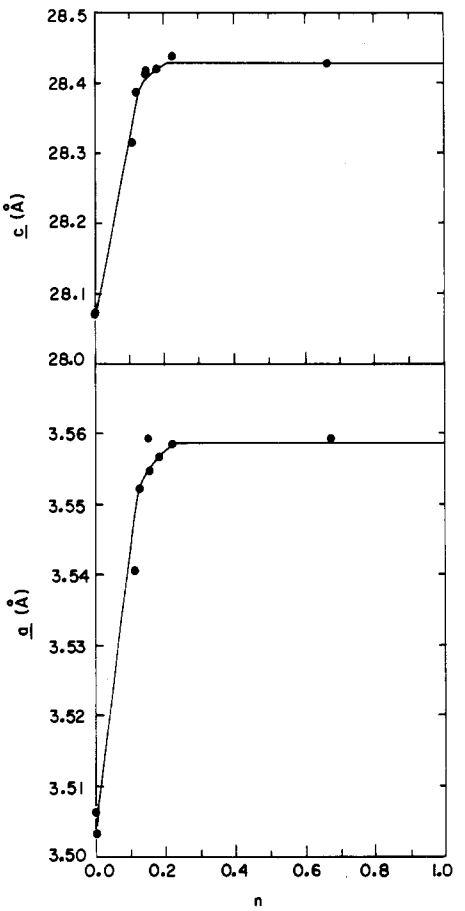

Figure 2. Lattice dimensions of the $ZrBr(O_y)$ product as a function of n for the reaction $ZrBr + nZrO_2 = ZrBr(O_y) + nZr(O_x)$.

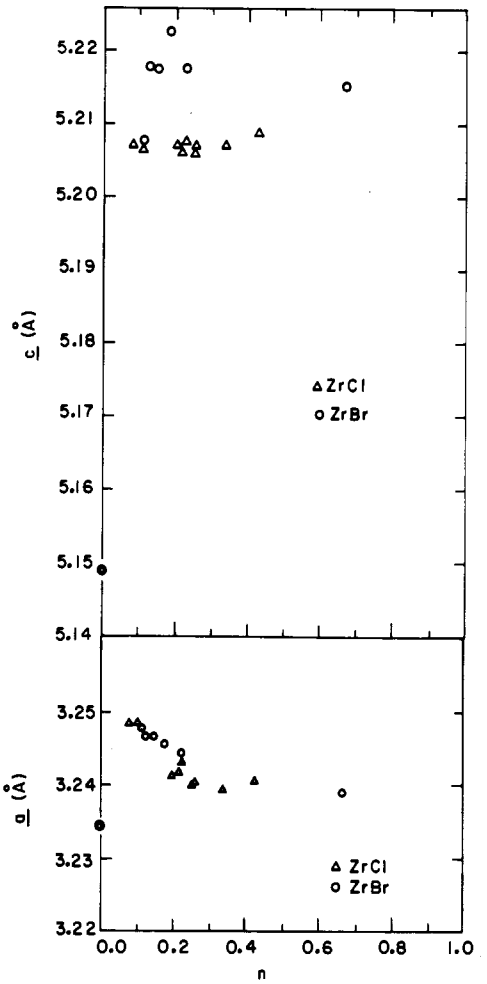

Figure 3. Lattice dimensions for the metal $Zr(O_x)$ coproduct of the reactions of ZrCl (Δ) and ZrBr (O) with $nZrO_2$.

and $ZrBr(O_y)$ products, respectively, and Figure 3 shows the corresponding lattice constant variations for the metallic coproduct $Zr(O_x)$ for both halide series. The breaks in Figures 1 and 2 define the ratio of reactants at which the above products reach equilibrium with ZrO_2. These correspond to $n = 0.27 \pm 0.01$ for the chloride according to changes in both a and c and a smaller 0.22 ± 0.02 for the more covalent bromide (0.23 from a and 0.21 from c).

The lattice dimension changes found for the metal product $Zr(O_x)$ (Figure 3) are much more meaningful when compared with the analogous information for solution of ZrO_2 in Zr in the absence of halide. These parameters have been determined by Guinier techniques by Holmberg and Dagerhamn[25] on arc-melted Zr/ZrO_2 mixtures that were subsequently annealed (in SiO_2) at various temperatures and quenched. In order to ensure that the apparent differences seen in Figure 3 did not arise from variations in the earlier preparations, an additional eight $Zr(O_x)$ compositions were prepared by isothermal equilibration at 930 °C. Their lattice dimensions (with standard deviations of (2–5) × 10^{-4} Å) are in excellent agreement with the earlier findings, as shown by the comparison in Figure 4. The general agreement shown by our results for samples prepared in tantalum also indicate there is no significant partition of oxygen from ZrO_x into the container. This is pertinent since a relatively small sample of ZrO_2 will turn gray (O:Zr ≥ 1.99:1) through reduction by the tantalum at 1000 °C.

The saturation composition indicated by Figure 4 is about $ZrO_{0.43}$ for the 800 and 930 °C data sets, which compares well with a $ZrO_{0.42}$ composition below about 1200 °C given by Ackerman et al.[26] The latter will be used hereafter. The very unusual shape of the dependence of the metal lattice dimensions on oxygen content is thought to arise from ordering reactions of the oxygen atoms to generate various superstructures.[27,28] One very weak extra line associated with these

(25) Holmberg, B.; Dagerhamn, T. *Acta Chem. Scand.* **1961**, *15*, 919.

(26) Ackerman, R. J.; Garg, S. P.; Rauh, E. G. *J. Am. Ceram. Soc.* **1977**, *60*, 341.

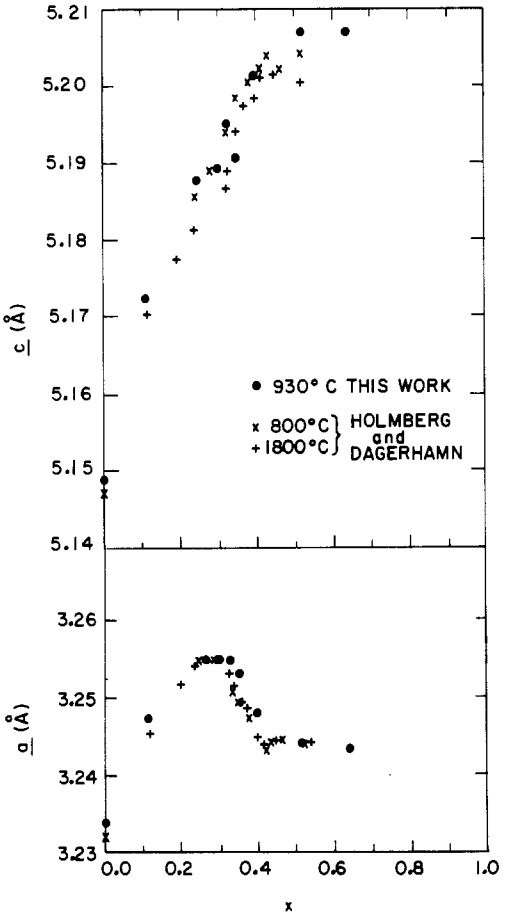

Figure 4. Hexagonal lattice dimensions of $Zr(O_x)$ formed from Zr and ZrO_2: O, this work; × and +, ref 25.

was observed in the Guinier patterns.

Two factors are evident in the metal phase $Zr(O_x)$ when this is generated by the monohalide reactions: a real and reversible effect of halide on the dimensions and a clearly unequal distribution of oxide between $ZrX(O_y)$ and $Zr(O_x)$ in systems not saturated with ZrO_2. The lattice constants for all phases in equilibrium with ZrO_2 are collected in Table III together with the percentage changes relative to ZrX or $Zr(O_x)$. Qualitatively, halide has the same (if any) effect on the lattice dimensions of $Zr(O_x)$ as does oxide alone near saturation, that is, decreasing a slightly and increasing c, although the latter change is puzzling in that only bromide seems to have an observable effect (0.012 (1) Å or 0.2%). The last is evident in the top part of Figure 3 as well. Microprobe examination did not reveal any chloride or bromide (at limits of about 0.2 and 0.04 atom %, respectively) in zirconium foils that had been equilibrated with excess ZrX and ZrO_2. Chloride appears to leave the $Zr(O_x)(X)$ phase fairly easily, presumably as $ZrCl_4$, as the lattice constants of the metal phase were found to revert to the values independently determined when an equilibrium mixture of $ZrCl(O_y)$ and $Zr(O_x)$ saturated with ZrO_2 was heated under high vacuum at 400 °C for a few hours, conditions under which the oxide is not mobile. More importantly, this demonstrates a negligible effect of chloride on oxide concentration at saturation. With present information, there is no way to judge whether the small concentration of bromide actually affects the oxide solubility in metal appreciably although an even smaller interstitial solubility would be expected on the basis of size. The effects of halide on dimensions of the pure metal have not been studied extensively, but these are very small, for example, a = 3.2328 (4) Å and c = 5.1505 (9) Å found for metal equilibrated with ZrCl at 1050 °C[14] compared with data for metal given in Table II.

The experiments designed to elucidate the stoichiometry of the reaction (Figures 1 and 2) are simultaneously much less suitable for estimating the oxygen partition between $ZrX(O_y)$ and $Zr(O_x)$ short of saturation, but it is evident that the metal phase is favored. Thus, according to the c lattice dimensions (Figure 3) all but one of the metal coproduct compositions obtained would appear to be saturated, or nearly so. The irregular effect of oxygen and the indefinite effect of halide on the a dimension at intermediate compositions make this measure more difficult to analyze quantitatively, but the data for both axes generally suggest that $Zr(O_x)$ is substantially saturated by roughly n = 0.12 (±0.04). Another experiment in which metal was added to a previously equilibrated $ZrCl/ZrO_2$ system at n = 0.23 to demonstrate the process was reversible actually gives more useful results. Here, the lattice dimensions for each phase indicate the halide phase corresponding to $n \sim 0.05$ is in equilibrium with $Zr(O_{\sim 0.24})$, that is 55–60% saturated according to Figure 4 if chloride has no significant effect at that point. The n = 0.11 data for $ZrBr/ZrO_2$, 50% of the ZrO_2 necessary for saturation, suggest that $ZrBr(O_y)$ is in equilibrium with $ZrO_{0.33}$ after some rough approximations are made regarding the effect of bromide on the latter's dimensions.

In the two cases just considered, y is roughly ~0.01 and ~0.1, respectively. But the lattice dimensions for the halide phases cannot be used directly to deduce y by interpolation because of both substantial positive deviation in that dependence and partial decomposition of the halide phases. The former can be deduced from single-crystal studies to be described later. An autogenous pressure of ZrX_4 from the decomposition

$$4ZrX(s) = 3Zr(s) + ZrX_4(g) \quad (2)$$

is to be expected, and this will presumably increase in the present studies first as the metal product is stabilized by oxide solution and as ZrX is somewhat more slowly oxidized to $ZrX(O_y)$. Pressures in (2) have been estimated to be 1 atm for both halides at 900 °C and 3 atm for ZrCl at the mean temperature (980 °C) of the present work.[4] The stoichiometry ratios n as weighed will therefore be altered, particularly for low n, by removal of both ZrX by decomposition and ZrO_2 by reaction with the metal produced. More importantly, the stoichiometric ratios n deduced at saturation (Figures 1 and 2) are actually only slightly lower than measured for $ZrCl_4$ pressures of 3–5 atm, the effect (0.01–0.02) therefore being comparable to their estimated uncertainties.

The coefficients in eq 1, which describe the ZrCl reaction with ZrO_2 at saturation, are fairly certain considering what is known about the stoichiometry of the products. A crystal structure study (below) confirms that the 1:1 ratio of Zr:Cl is retained in the product and that y at saturation is 0.43 with a standard deviation of 0.02. The former fixes the coefficient of $Zr(O_x)$ at that of ZrO_2, n. And use of a saturated composition for $Zr(O_x)$ unaltered by the presence of chloride turns out to be completely consistent with the oxygen conservation condition, making the chloride reaction with excess ZrO_2 at about 980 °C

$$ZrCl + 0.27ZrO_2 \rightarrow ZrCl(O_{0.43}) + 0.27Zr(O_{0.42}) \quad (3)$$

A structural solution for the oxygen content in the saturated bromide is not available, but assumption of an unaltered oxygen content in the metal phase (in spite of the evident effect that bromide has on the c dimension) gives

$$ZrBr + 0.22ZrO_2 = ZrBr(O_{0.35}) + 0.22Zr(O_{0.42}) \quad (4)$$

(27) Yamaguchi, S. *J. Phys. Soc. Jpn.* **1968**, *24*, 855.
(28) Fehlmann, M.; Jostons, A.; Napier, J. G. *Z. Kristallogr.* **1969**, *129*, 318.

Table IV. Refined Crystal Parameters for Zirconium Monohalide Oxide Phases (Space Group $R\bar{3}m$)

	$ZrCl$[a]	$ZrClO_{0.29}$	$ZrClO_{0.43}$	$ZrBr$[b]	$ZrBrO_{0.23}$
a, Å	3.4233 (5)	3.4926 (3)	3.4984 (2)	3.5031 (3)	3.5594 (4)
c, Å	26.693 (3)	27.025 (8)	27.065 (4)	28.071 (3)	28.418 (5)
z(Zr)	0.1221 (1)	0.12111 (9)	0.12084 (4)	0.2092 (4)	0.2092 (2)
z(X)	0.3901 (3)	0.3897 (3)	0.3895 (1)	0.3917 (5)	0.3903 (2)
z(O)		0.202 (2)	0.2001 (6)		0.135[c]
B_{11}(Zr)	0.4 (2)	0.56 (7)	1.58 (4)	0.5 (4)	1.3 (2)
B_{33}(Zr)	0.51 (4)	0.4 (1)	1.72 (5)		0.7 (3)
B_{11}(X)	0.6 (3)	0.7 (2)	1.63 (6)	1.9 (4)	1.3 (2)
B_{33}(X)	0.52 (6)	0.7 (2)	1.85 (9)		0.7 (3)
B(O)		0.7[d]	1.5 (3)		0.7[d]
occupancy (O)		0.29 (4)	0.43 (2)		0.23[c]
R		0.059	0.046		0.092
R_w		0.084	0.056		0.183
2θ limit, deg		50	60		50
no. of reflcns		86	141		102

[a] References 3 and 4; $x = y = 0$. [b] Refined powder data with isotropic thermal parameters; from ref 4. [c] Estimated from Fourier map phased with Zr and Br. [d] Fixed parameters.

The small amount of chloride found in the ZrO_2 reactant after these reaction studies had been completed is not particularly significant. For example, the higher of the two determinations (see Experimental Section) has a much smaller effect than does the uncertainty in either the experimental n (0.01) or y (0.02) value for the chloride, and eq 3 remains the best description. Though the bromide product in (4) contained ~2% chloride (semiquantitatively confirmed by microprobe), the results are not changed in any significant way, especially in view of the fact that n is more uncertain (0.02) and y = 0.35 is only an inferred value.

Reactions of ZrCl with $ZrS_{1\pm x}$, ZrC, ZrN, or ZrF_4 in the range of 900–1000 °C (see Experimental Section for conditions) gave no hint of significant non-metal introduction into ZrCl on the basis of changes in lattice dimensions. The monochloride was found to reduce Zr_xS (NaCl) to ZrS_{1-x} (WC) and to be effective in scavenging oxygen (as $ZrCl(O_y)$) from impure ZrS_2 or ZrN. The latter effect was verified on a single crystal of the sulfide product by X-ray means ($ZrCl(O_{0.29})$), while a substantial oxygen surface impurity on the ZrN reactant was established by XPS measurements and the product crystals were identified by Guinier data. Our values for the lattice dimensions of the metal phase $ZrN_{\sim 0.29}$ in equilibrium with ZrN at 1000 °C[29] are 3.2584 (4) and 5.226 (1) Å, appropriately larger than those of the oxide (see Discussion), while those for metal saturated with ZrF_4 at 950 °C are 3.2443 (2) and 5.1690 (5) Å, equivalent to about $ZrO_{0.08}$ in Figure 4.

Structural Determinations. Three refinements of the X-ray structures of single crystals of $ZrCl(O_y)$ and one of $ZrBr(O_y)$ were carried out. Data for two chloride oxides, a bromide oxide, and the two ZrX parents are summarized in Table IV. The refinements started with the parameters of the corresponding ZrX phase because of the obvious close relationship (see Experimental Section), and these quickly revealed the bound oxygen in a tetrahedral interstice between the metal layers. Both the positional and occupational parameters for oxygen could be varied only with the chloride $ZrCl(O_{0.43})$ isolated from a saturated system; the oxygen content was also confirmed (±50%) by microprobe. At the other extreme, the heavier bromide and an evidently poorer crystal made the oxygen refinement less well conditioned, the atom coordinates wandering to a point outside the metal double layers where no density was evident on electron density or difference electron density maps. As a result, the electron density map phased with the heavy atoms was used to deduce the oxygen's position and occupancy (0.23), the latter from the integrated peak height relative to those of the heavy atoms. The chloride crystal structure not reported in the table had the lowest oxygen content (0.25 ± 0.05) and did not refine very well (R

Table V. Some Comparative Distances (Å) in ZrX and $ZrX(O_y)$

	y for $ZrCl(O_y)$			y for $ZrBr(O_y)$	
	0[a]	0.29	0.43	0[a]	0.23[b]
Zr–Zr[c]	3.087 (5)	3.183 (4)	3.199 (2)	3.130 (12)	3.173 (6)
Zr_A–O[d]		2.19 (7)	2.15 (2)		2.10
Zr_B–O[d]		2.035 (10)	2.047 (3)		2.08
Zr–X	2.629 (6)	2.669 (5)	2.673 (2)	2.74 (1)	2.805 (5)
X–O		2.85 (5)	2.90 (1)		3.03
X–X[c]	3.61 (1)	3.65 (1)	3.648 (5)	3.85 (2)	3.84 (1)
O–O[e]		2.78 (10)	2.71 (3)		2.73

[a] References 3 and 4. [b] Oxygen position estimated (see Table IV). [c] Interlayer distances; the intralayer distances Zr–Zr and X–X are the a dimension (Table IV). [d] Zr_A is the apex and Zr_B the base, as designated in Figure 6. [e] Interlayer distance.

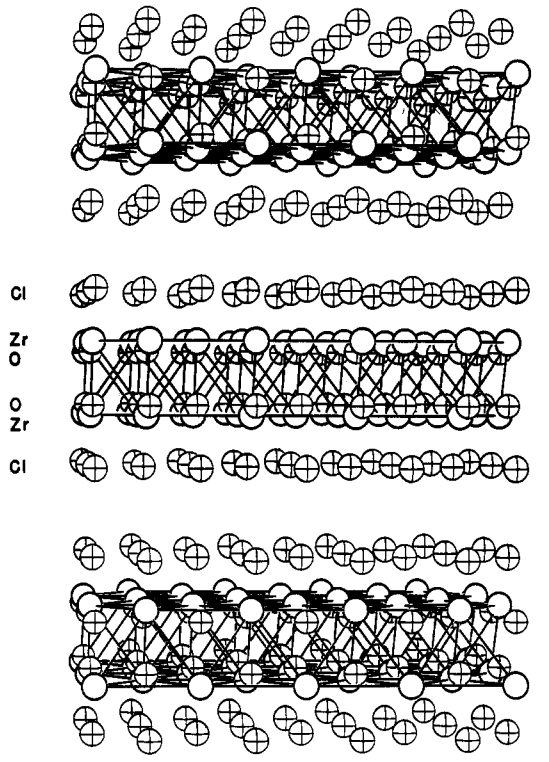

Figure 5. A section of the three-slab structure of $ZrCl(O_{0.43})$, with oxygen randomly distributed in 43% of the tetrahedral holes between the double zirconium layers. The c axis is vertical (95% thermal ellipsoids).

(29) Domagala, R. F.; McPherson, D. J.; Hansen, M. *Trans. Am. Inst. Min., Metall. Pet. Eng.* **1956**, *206*, 98.

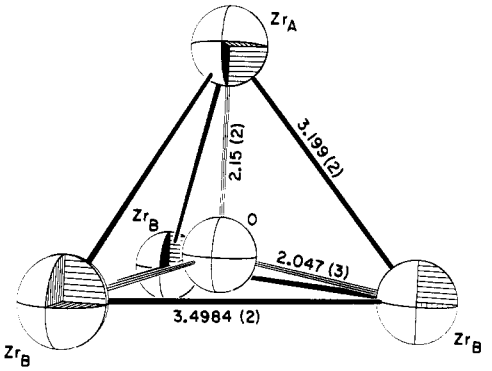

Figure 6. The Zr_4O unit and dimensions in $ZrCl(O_{0.43})$. Zr_A and Zr_B lie in separate metal layers.

= 0.08, R_w = 0.12), the ratio of about 3 for the thermal ellipsoids B_{33}/B_{11} being common evidence for stacking defects in these layered compounds.

Important distances in the three structures are listed in Table V. A view of a portion of the structure of $ZrClO_{0.43}$ is given in Figure 5, while the OZr_4 group therein is shown in Figure 6 with the pertinent distances. The metal tetrahedra in all phases are compressed in this manner with edges that differ by 0.30–0.38 Å. The increase in Zr–Zr distances on oxygen substitution seems fairly reasonable. However, the increase in the Zr–Cl distance between ZrCl and $ZrCl(O_{0.43})$ appears to point to significant O–Cl repulsion, the separation of these two atoms in the oxidized phase (2.90 Å) being significantly less than the van der Waals sum, ~3.2 Å.[30]

Surprisingly, no X-ray evidence of oxygen ordering in $ZrCl(O_{0.43})$ could be found, even on slowly cooled samples, in contrast to the behavior of $Zr(O_{0.42})$. The 2.71-Å distance between neighboring oxygen atoms in the two layers of oxygen in each slab (see Figure 6) vs. nearly 3.50 Å within each layer suggests that preferential occupation of a single layer might take place as the occupation approaches 50%. However, the result of this would be polar, a disadvantage. If any such ordering does take place at 43% occupancy, it must occur only in small domain regions.

Photoelectron Studies. As shown in Figure 7, the UPS spectrum of the valence region for $ZrClO_{0.43}$ relative to that for ZrCl gives an immediate reflection of valence-bonding changes brought on by oxide substitution. Both give obvious Fermi edges, somewhat greater for the clearly metallic $ZrCl(O_{0.43})$. The shoulder at ~8 eV presumably marks the oxide contribution, while the negative shift of the chlorine 3p binding energy by 0.3 eV probably means that E_F comes down on oxidation. The small amount of the chloride oxide available prevented measurement of a satisfactory XPS valence spectrum because of significant interference from the indium mounting. Relevant core peaks measured were Zr $3d_{5/2}$ 179.9 eV, Cl $2p_{3/2}$ 199.9 eV, and O 1s 530.6 eV. The zirconium core binding energy in $ZrClO_{0.43}$, 0.5 eV greater than that for ZrCl, is quite appropriate for an oxidation state of +1.86 when compared with data for other zirconium chlorides.[13,31]

Discussion

The Oxide Reactions. Our research on the reduced zirconium halides over the past decade has never been troubled by the formation of recognizable oxyhalides even though the ubiquitous oxygen makes itself so very evident as oxyhalides of elements in neighboring groups, scandium and yttrium for example.[32] This can be understood at least partially now that

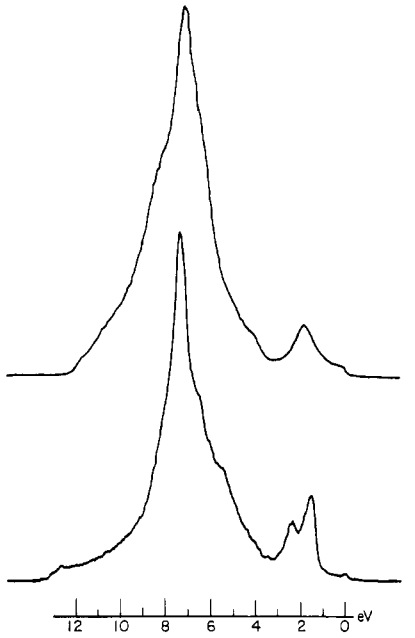

Figure 7. Ultraviolet (He I) photoemission spectra of the valence region of $ZrCl(O_{0.43})$ (top) and ZrCl (bottom). The binding energy (eV) is referenced to the Fermi level at zero.

the unusual ability of the metallic ZrCl and ZrBr to take up oxide interstitially has been discovered.[33] The saturation limits of $ZrCl(O_{0.43})$ and $ZrBr(O_{\sim 0.35})$ are in fact remarkably similar to that of the metal, $Zr(O_{0.42})$. The known HfCl, which is isostructural with ZrBr,[4,34] presumably forms an analogous oxide. On the other hand, the lowest titanium dihalides occur only in traditional structures (CdX_2 type) and form likewise conventional oxyhalides[35] owing to a sharply restricted ability to form strong metal–metal bonds. Why only group 4 elements among the transition elements share this distinctive characteristic of massive oxygen solution is not at all obvious although, as discussed below, suitably sized interstices and the relative stability of the neighboring oxide phase must be important.

Although single-phase $ZrX(O_y)$ phases could presumably be obtained by careful, direct reaction of oxygen with the monohalides followed by suitable annealing, the character of the ZrX–ZrO_2 reaction studied better reflects some remarkable chemical changes, viz.

$$ZrX + nZrO_2 \rightarrow ZrX(O_y) + nZr(O_x)$$

with x and y increasing (x more rapidly at first) toward saturation with increasing n. Because the ZrX layers are preserved, production of a second zirconium phase is required, and the reaction can be interpreted as the reduction of ZrO_2 to the equivalent amount of oxygenated metal, the ZrX in turn being oxidized to $ZrX(O_y)$. Implicit in this description is the particular driving force provided by (stability of) the other product, $Zr(O_x)$. Of course, the reaction can also be described in terms of the disproportionation of ZrX by ZrO_2, with the same conclusion. The products of the reaction of ZrX with silica at 850 °C for a few days give broad and evidently

(30) Pauling, L. "The Nature of the Chemical Bond", 3rd ed.: Cornell University Press: Ithaca, NY, 1960; p 260.
(31) Corbett, J. D. *Inorg. Chem.* **1983**, *22*, 2669.
(32) Ford, J. E.; Hwu, S.-J.; Ziebarth, R. P.; Corbett, J. D., unpublished research, 1982.
(33) The c lattice constant for ZrBr has been reported to vary from 28.06 (1) to 28.40 Å for samples prepared in SiO_2 and, by implication, for ZrCl as well (Troyanov, S. I.; Marek, G. S.; Tsirel'nikov, V. I. *Russ. J. Inorg. Chem. (Engl. Transl.)* **1973**, *18*, 135). This must result from the formation of these $ZrX(O_y)$ compositions under some conditions. We have been unable to detect any evidence for nonstoichiometry of the binary monohalides by Guinier techniques.[4]
(34) Struss, A. W.; Corbett, J. D. *Inorg. Chem.* **1970**, *9*, 1373.
(35) Wells, A. F. "Structural Inorganic Chemistry", 4th ed.; Oxford University Press: London, 1975.

analogous X-ray patterns of $ZrX(O_y)$, presumably mixed with an unidentified zirconium silicide.

Bonding. The insertion of oxygen into the electron-rich region between the metal layers in ZrX results in removal of two electrons from the metal–metal bonds (valence band) and the formation of oxide-like states with 2p binding energies in the neighborhood of halide (7–8 eV relative to E_F). Some covalent contribution to the binding of oxide to metal is expected so that a completely ionic picture of the oxide state is not appropriate, although the covalent mixing between the metal and halide valence bands in the parent ZrX does appear modest. The corresponding description of the changes taking place on formation of the ZrXH phases is very analogous.[11] The oxidation of ZrX is accompanied by a small expansion within the layers and a somewhat larger expansion between the metal layers where the Zr–Zr distances were initially smaller. The bromide has somewhat greater Zr–Zr distances to begin with, and these show less relative expansion. Pauling metal–metal bond order totals (0.82 per electron pair in ZrCl and 0.66 in ZrBr[36]) show only small changes (by −5 and +3%) at the highest compositions studied with single crystals (Table V), meaning that the expansion is more or less appropriate to the degree of oxidation. Of course, some metal–metal bonding between the two zirconium layers is replaced by coulombic and covalent Zr–O bonding and core repulsion, and the relevant question of interstice and oxygen size will be considered later. Were the oxide in $ZrX(O_y)$ to reach full occupancy ($y = 1$), the structure for chloride and bromide would correspond to that of the normal-valent SmSI and YOF,[37] respectively.

The inability to form more conventional intercalation derivatives M^I_xZrCl through addition of x electrons to the inter-zirconium region together with alkali-metal cations in the van der Waals gap between the chlorine layers now seems well established. Other reactants appear to provide hydrogen too readily and allow the formation of the stable $ZrXH_x$ phases (see Table I). The instability of these intercalates must relate to the already high electron density in the inter-metal region since intercalated alkali-metal derivatives of the d^2 YCl have been obtained.[38] On the other hand, the analogous $YCl(O_y)$, $y << 1$, does not exist, probably because of the high stability of YOCl. No other zirconium oxychlorides are known (unless hydrated).

Interstitial Sizes and Site Preferences. Volume properties appear to be quite important not only in these phases but also in many other so-called interstitial or α-phase solutions of non-metals in metals. The size effects are most easily seen in the quite self-consistent non-metal radii or metal–non-metal distances exhibited in these phases. A general theme appears to be developing regarding oxidized vs. reduced phases: that metal-binding electrons are not a major factor in screening the metal–non-metal interactions—indeed the electrons should avoid the somewhat negative non-metal region—and that the metal–non-metal separations in a homologous series turn out to be about the same as long as localized metal states do not intrude. Thus, 2.58 ± 0.05 Å spans the observed Zr–Cl distances in ZrCl, $ZrCl_2$, ZrClH, $K_2Zr_7Cl_{18}$, and $ZrCl_3$. The sum of six-coordinate crystal radii[39] for chloride and the zirconium(IV) core, 2.53 Å, is in good agreement with observation. Of course the actual coordination numbers of zirconium and chloride in these are different (usually less) and variable, but the somewhat arbitrary choice of six-coordinate references works relatively well. Similar close correspondence to standard radii has been noted in the metal-chain structures of scandium and yttrium chlorides[40] and with many metallic hydrides.[11] Some deviations may still arise with unusual coordination numbers, and what has been termed covalent shortening[39] is apt to be found with high oxidation states, e.g., in $ZrCl_4$.

Table VI. Mean Radii of Tetrahedral-like and Octahedral-like Interstitial Sites in Some Metallic Zirconium Phases and the Corresponding Crystal Radius Sums (Å)

phase	site radius tet	site radius oct	obsd occupancy
Zr	1.96	2.27	
$ZrO_{0.42}$	1.98	2.28	O_h
$ZrH_{0.01}$ [a]	1.96	2.27	T_d
$ZrN_{0.37}$	1.98	2.29	O_h?
ZrCl	2.01	2.31	
$ZrClO_{0.43}$	2.06	2.37	T_d
ZrBr	2.05	2.35	
$ZrBrO_{\sim 0.23}$	2.08	2.38	T_d

atoms	radius sum[b] tet	radius sum[b] oct	atoms	radius sum[b] tet	radius sum[b] oct
Zr, O	2.10	2.12	Zr, F	2.03	2.05
Zr, H[c]	1.96		Zr, Cl		2.53
Zr, N	2.18				

[a] Reference 43. [b] Radii for six-coordinate Zr and the indicated CN for the non-metal, ref 39. [c] Hydrogen value (1.10 Å) from ref 11.

The Zr–O distances in $ZrCl(O_{0.43})$ (Figure 6) are also in accord with the foregoing even though the non-metal now intrudes into the electron-rich region. The average value, 2.07 Å, compares favorably both with 2.10 Å for the sum of crystal radii for six-coordinate Zr and four-coordinate O[39] and with 2.065 and 2.090 Å for the shorter Zr–O distances in tetragonal[41] and monoclinic[42] ZrO_2 for four- and three-coordinate oxygen, respectively. The oxides of course exhibit zirconium coordinate polyhedra very different from those considered here. The fact that the Zr–O distances in $ZrClO_{0.43}$ are about as short as found anywhere is in accord with the volume changes observed during formation.

In the foregoing terms the choice of a tetrahedral site for oxygen in $ZrX(O_y)$ but an octahedral one in $Zr(O_x)$ seems to be mainly a matter of relative size as best as these can be judged. Data for the observed mean radii of both tetrahedral- and octahedral-type interstices in these and related phases together with the corresponding crystal radii sums are given in Table VI. When these are considered in a relative sense, the octahedral holes in ZrX seem too large for a reasonably bound oxygen and, conversely, the tetrahedral sites appear too small in the metallic phase. Radii of the octahedral interstices in the metal are in fact not very different from the Zr–O distances in cubic ZrO_2, 2.27 vs. 2.20 Å.[35] Actually the idealized "fit" of oxygen in tetrahedral holes in ZrX may be somewhat "tight" (Table VI), and a larger expansion of the interstices is seen during oxidation of ZrX than with the metal. The first circumstance may not be as serious for distorted tetrahedra such as these with 9–12% differences in edge dimensions while other evidence bearing on the expansion will be considered shortly.

Our inability to substitute nitride or carbide into the *tetrahedral* interstices in the ZrCl structure by analogous reactions with ZrN or ZrC appears to arise from the non-metal's greater size with respect to oxide although thermodynamic unfavorability (a restatement of sorts) or kinetic inhibitions

(36) Corbett, J. D. *J. Solid State Chem.* **1981**, *37*, 335.
(37) Hullinger, F. In "Structural Chemistry of Layer-type Phases"; Levy, F., Ed.; D. Reidel Publishing Co.: Boston, MA, 1976; Chapter IV, Section 14.
(38) Ford, J. E.; Corbett, J. D.; Hwu, S.-J. *Inorg. Chem.* **1983**, *22*, 2789.
(39) Shannon, R. D. *Acta Crystallogr., Sect. A* **1976**, *A32*, 751.
(40) Corbett, J. D. *Acc. Chem. Res.* **1981**, *14*, 239.
(41) Teuffer, G. *Acta Crystallogr.* **1962**, *15*, 1187.
(42) Smith, D. K.; Newkirk, H. W. *Acta Crystallogr.* **1965**, *18*, 983.
(43) Beck, R. L. *ASM Trans. Q.* **1962**, *55*, 556.

could also account for the negative results. Although the trigonally compressed "octahedral" sites in ZrCl would seem more suitable sites, the non-metal would then have two halides at 2.93 Å as second-nearest neighbors in the ccp slabs. This distance appears well less than probable van der Waals sums (>3.3 Å[30]) but is not very different from oxygen–chlorine separations around the tetrahedral hole (Table V) where a repulsion may be inferred. In fact, a rearranged slab (AbaB) does accommodate carbon in the octahedral site in 1T-Zr_2X_2C, X = Cl, Br.[32,38] Mass transfer does not seem to be a likely barrier to reaction of ZrF_4 in view of its obvious volatility at temperature and neither does a size restriction (Table VI). But a second product is required by the reaction stoichiometry (eq 1), and in this case a favorable solution of fluoride in the metal analogous to that of the oxide[44] does not appear to be significant.

A distinctly larger expansion of the metal polyhedra takes place on oxidation of ZrX phases than with the stoichiometrically (and electronically) similar oxidation of the metal to $Zr(O_{0.42})$. Thus, the expansion of the metal volume is 1.89% to $Zr(O_{0.42})$, or 2.17% at the maximum in *a* (Figure 4) before onset of the contraction associated with ordering, while conversion of ZrX to $ZrX(O_{0.43})$ involves an overall volume increase of 5.9% (Cl) to 4.5% (Br), or 8.9% in the chloride when just the volume of the subcell between the two metal layers is considered. Naturally the available interstitial volume in YCl is greater, and so only a 3.9% expansion in the comparable inter-metal subcell is necessary for conversion to $K_{0.08}YCl(O_{0.8})$.[38] In addition, the $Zr(O_x)$ solution exhibits a fair approximation to Vegard's rule up to about $x = 0.20$; that is, the lattice constants vary linearly with composition,[25] while those (and the cell volumes) of ZrCl and the three single crystals of $ZrCl(O_y)$ studied show substantial positive deviation from linearity with y. This appears to be further evidence of an expansion that is forced on the interlayer separation in the early stages, somewhat analogous to (but smaller than) that seen on the one-phase intercalation of lithium into MS_2 to form Li_xTiS_2 or Li_xTaS_2 where the initial "spacers" cause a relatively large change in the interslab separation.[45] Again, the coproduction of $Zr(O_x)$ may provide a significant driving force.

Acknowledgment. We thank F. Laabs, E. DeKalb, and J. Anderegg for their assistance in analyses. R. A. Jacobson and co-workers provided valuable assistance in the crystallographic portion of the study, while R. L. Daake and H. Imoto prepared most of the zirconium monohalide samples used.

Supplementary Material Available: Tables of structure factor amplitudes (3 pages). Ordering information is given on any current masthead page.

(44) Ackerman, R. J.; Garg, S. P.; Rauh, E. G. *High Temp. Sci.* **1979**, *11*, 199.

(45) Whittingham, M. S. *Prog. Solid State Chem.* **1978**, *12*, 47, 53.

Contribution from the Department of Chemistry, Case Western Reserve University, Cleveland, Ohio 44106

Copper(II) Complexes with Tetradentate Bis(pyridyl)–Dithioether and Bis(pyridyl)–Diamine Ligands. Effect of Thioether Donors on the Electronic Absorption Spectra, Redox Behavior, and EPR Parameters of Copper(II) Complexes

D. E. NIKLES, M. J. POWERS, and F. L. URBACH*

Received April 21, 1982

Eight copper(II) chelates containing a tetradentate bis(pyridyl)–dithioether ligand, $py(CH_2)_xS(CH_2)_yS(CH_2)_xpy$, or a bis(pyridyl)–diamine ligand, $py(CH_2)_xN(R)(CH_2)_yN(R)(CH_2)_xpy$, where $x = 1$ or 2, $y = 2$ or 3, and R = H or CH_3, were studied to determine the effect of thioether donors on the spectral and redox properties of the copper complexes. The systematic variation of the chelate ring sizes (5–5–5, 5–6–5, 6–5–6, and 6–6–6) allowed stereochemical trends in the observed properties to be ascertained as well as the effect of thioether substitution for the amine donors. The electronic absorption spectra of the $Cu^{II}[(py)_2S_2]$ complexes differed from those of the $Cu^{II}[(py)_2N_2]$ series by the presence of a $S(\sigma) \rightarrow Cu(II)$ LMCT in the near-ultraviolet region and an enhanced intensity in the visible (d–d) bands which was attributed to an intensity-borrowing mechanism from the low-energy charge-transfer band. The Cu(I) complexes of both series of ligands exhibited an absorption band between 300 and 350 nm corresponding to a $Cu(I) \rightarrow py(\pi^*)$ MLCT transition. The Cu(II)/Cu(I) reduction potentials for the chelates typically showed little solvent dependence in acetonitrile and aqueous solutions as measured by cyclic and differential pulse voltammetry. The potentials for the $(py)_2S_2$ series spanned a range ($E^{\circ\prime}$ = +400 to +660 mV vs. NHE) substantially higher than those exhibited by the $(py)_2N_2$ series ($E^{\circ\prime}$ = −170 to +320 mV vs. NHE). The substitution of two thioether donors for two amine donors produced an increase in $E^{\circ\prime}$ of 300–700 mV in pairs of the $(py)_2S_2$ and $(py)_2N_2$ complexes with the same chelate ring sizes. The reduction potentials for both series increase with increasing chelate ring size, suggesting that the larger chelate rings can more readily accommodate a pseudotetrahedral Cu(I) form. The anisotropic EPR parameters for the $Cu^{II}[(py)_2N_2]$ series were nearly axial while the $Cu^{II}[(py)_2S_2]$ series exhibited rhombic spectra representing the reduction in the effective donor atom symmetry of the complexes when the amine donors were replaced with thioether donors.

Introduction

With advances in the study of "blue" copper proteins there has been much interest in the spectroscopic features associated with copper–sulfur coordination. Recent X-ray crystal structures[1] of poplar plastocyanin and azurin indicate that the coordination sphere of the "blue" copper consists of a methionine thioether, a cysteine mercaptide, and two histidine imidazole ligands. This result substantiated the growing spectral evidence for a distorted-tetrahedral geometry[2-4] and

(1) (a) Coleman, P. M.; Freeman, H. C.; Guss, J. M.; Murata, M.; Norris, V. A.; Ramshaw, J. A. M.; Venkatappa, M. P. *Nature (London)* **1978**, *272*, 319. (b) Adamn, E. T.; Stenkamp, R. E.; Sieker, L. C.; Jensen, L. H. *J. Mol. Biol.* **1978**, *125*, 35. (c) Freeman, H. C. In "Coordination Chemistry-21"; Laurent, J. P., Ed.; Pergamon Press: New York, 1981; p 29.

(2) Gray, H. B.; Solomon, E. I. In "Copper Proteins"; Spiro, T. G., Ed.; Wiley-Interscience: New York, 1981; p 1.

(3) (a) McMillin, D. R.; Holwerda, R. A.; Gray, H. B. *Proc. Natl. Acad. Sci. U.S.A.* **1974**, *71*, 1339. (b) McMillan, D. R.; Rosenberg, R. C.; Gray, H. B. *Ibid.* **1974**, *71*, 4760.

(4) Solomon, E. I.; Rawlings, J.; McMillin, D. R.; Stephens, P. J.; Gray, H. B. *J. Am. Chem. Soc.* **1976**, *98*, 8046.

0020-1669/83/1322-3210$01.50/0